Available online at www.sciencedirect.com
SCIENCE DIRECT
Bioorganic & Medicinal Chemistry
ELSEVIER
Bioorganic & Medicinal Chemistry 14 (2006) 1506–1517

Direct observation (NMR) of the efficacy of glucagon receptor antagonists in murine liver expressing the human glucagon receptor

Sheila M. Cohen,[a] Joseph L. Duffy,[b,*] Corin Miller,[a] Brian A. Kirk,[b] Mari Rios Candelore,[c] Victor D. H. Ding,[c] Gregory Kaczorowski,[d] Laurie M. Tota,[c] Jeffrey G. Werrmann,[a] Michael Wright,[c] Emma R. Parmee,[b] James R. Tata[b] and Bei B. Zhang[c]

[a]*Department of Research Imaging, Merck Research Laboratories, Rahway, NJ 07065, USA*
[b]*Department of Medicinal Chemistry, Merck Research Laboratories, Rahway, NJ 07065, USA*
[c]*Department of Molecular Endocrinology, Merck Research Laboratories, Rahway, NJ 07065, USA*
[d]*Department of Biochemistry and Physiology, Merck Research Laboratories, Rahway, NJ 07065, USA*

Received 5 July 2005; revised 3 October 2005; accepted 3 October 2005
Available online 25 October 2005

Abstract—The demonstration of pharmacodynamic efficacy of novel chemical entities represents a formidable challenge in the early exploration of synthetic lead classes. Here, we demonstrate a technique to validate the biological efficacy of novel antagonists of the human glucagon receptor (hGCGR) in the surgically removed perfused liver prior to the optimization of the pharmacokinetic properties of the compounds. The technique involves the direct observation by ^{13}C NMR of the biosynthesis of [^{13}C]glycogen from [^{13}C]pyruvate via the gluconeogenic pathway. The rapid breakdown of [^{13}C]glycogen (glycogenolysis) following the addition of 50 pM exogenous glucagon is then monitored in real time in the perfused liver by ^{13}C NMR. The concentration-dependent inhibition of glucagon-mediated glycogenolysis is demonstrated for both the peptidyl glucagon receptor antagonist **1** and structurally diverse synthetic antagonists **2**–**7**. Perfused livers were obtained from a transgenic mouse strain that exclusively expresses the functional human glucagon receptor, conferring human relevance to the activity observed with glucagon receptor antagonists. This technique does not provide adequate quantitative precision for the comparative ranking of active compounds, but does afford physiological evidence of efficacy in the early development of a chemical series of antagonists.
© 2005 Elsevier Ltd. All rights reserved.

1. Introduction

Diabetes mellitus is a condition characterized by chronically elevated levels of blood glucose. This condition arises from inappropriate secretion and activity of the two major pancreatic hormones that control glucose homeostasis, insulin and glucagon. In the diabetic state, insulin resistance and insulin deficiency impair the body's ability to absorb and utilize glucose from the bloodstream. The condition is commonly aggravated by chronically elevated levels of the peptide glucagon or hyperglucagonemia.[1] Glucagon is a 29 amino acid peptide that is released from pancreatic α cells. In healthy individuals, the hormone is synthesized and secreted in response to insufficient plasma glucose levels. The peptide activates the hepatic glucagon receptor (GCGR) and triggers the synthesis of glucose (gluconeogenesis) and processing and release of hepatic glycogen stores (glycogenolysis) to restore plasma glucose and maintain homeostasis. In diabetic individuals, inappropriately high hepatic glucose production arising from elevated glucagon exacerbates inappropriately low glucose utilization. The combination of these two deficiencies results in chronic hyperglycemia. Many therapeutic approaches to the treatment of diabetes have focused on the normalization and utilization of plasma insulin.[1c,2] An alternative or additional therapy may be realized by blocking hepatic glucose production using glucagon receptor antagonists.[3] Peptidyl antagonists are known,[4] and several small molecule synthetic antagonists have been reported as well.[5]

The activity of peptide or small molecule glucagon receptor antagonists may be readily measured at the cellular level with in vitro receptor binding and functional

Keywords: Glucagon; Antagonist; Glycogenolysis; Perfused liver; Diabetes; NMR; Transgenic.
* Corresponding author. Tel.: +1 732 594 1062; fax: +1 732 594 5350; e-mail: joseph_duffy@merck.com

0968-0896/$ - see front matter © 2005 Elsevier Ltd. All rights reserved.
doi:10.1016/j.bmc.2005.10.008

assays. The antagonists may be further investigated in vivo using a variety of animal models of diabetes mellitus. However, the demonstration of pharmacodynamic efficacy requires that the compound be optimized beyond intrinsic potency to overcome several additional obstacles to an interpretable experiment. For example, the investigational compound must be sufficiently potent on the glucagon receptor that is endogenous to the animal model. In the event that the antagonist is highly potent against the human receptor, but lacks potency against other mammalian receptor variants, the probability of demonstrating a pharmacological effect in other species is low. Indeed, in early reports from these laboratories we observed a variable but substantial decrease in the binding affinity of glucagon receptor antagonists in the murine receptor.[9b] Additionally, the pharmacokinetic parameters of the compound must be suitable for the route of administration, such that the compound can reach sufficient concentration in hepatic tissue to exert a measurable physiological response. The optimization of these parameters may add substantial additional barriers to the early demonstration of efficacy of a given lead class of glucagon receptor antagonists.

In previous reports from these laboratories, we addressed the species-dependent receptor variation with the development and characterization of a strain of transgenic mice that express the human glucagon receptor.[6] The homozygous receptor replacement mice (hGCGR mice) were healthy and fertile, and employ a human hepatic glucagon receptor that was demonstrated to be functionally intact both in vitro and in vivo. The utilization of hGCGR mice allows for a meaningful correlation of murine hepatic gluconeogenic activity with in vitro potency of antagonists optimized against the human glucagon receptor.

The challenge of attaining sufficient in vivo compound exposure for validation of efficacy may be overcome by examining the activity of compounds in the entire functioning organ ex vivo. The mouse liver is an attractive candidate organ for ex vivo study by NMR spectroscopy owing to its surgical accessibility and small size.[7] With the infusion of ^{13}C-labeled pyruvate into a surgically removed and perfused murine liver, we have monitored the biosynthesis of glycogen in real time by perfused-liver ^{13}C NMR and observed the rapid breakdown of glycogen in response to exogenously administered glucagon. An NMR spectrometer equipped with a standard vertical-bore NMR magnet was used for these studies.[8]

Herein we report that the time-resolved perfused-liver NMR technique may be used for the direct observation of the inhibition of glucagon-induced glycogenolysis by glucagon receptor antagonists. We have employed perfused liver from the murine hGCGR replacement strain to minimize species-dependent differences in the efficacy of the antagonists and to confer human relevance to the experiments. We examined a structurally diverse set of small molecule glucagon receptor antagonists at multiple concentrations for the ability to inhibit glucagon-induced glycogenolysis in the perfused hGCGR liver. The efficacy of these compounds in this whole organ assay was compared with the intrinsic potency observed in the in vitro functional (cAMP) assay to examine the pharmacodynamic relevance of gains in intrinsic potency.

2. Results

2.1. Chemistry

The glucagon receptor antagonists investigated in the present study are illustrated in Table 1. The peptidyl antagonist **1**,[4a] the triarylpyrrole antagonist **2**,[9] and the 4-phenylpyridine antagonists **6** and **7** have been reported previously.[10] Recently, we reported the discovery of the thiophene-derived glucagon receptor antagonists **3** and **4**, and an inactive variant of these compounds **5**, in brief communications.[11] The synthesis of the cyclohexyl substituted thiophenes **3** and **5** is illustrated in Scheme 1. The cyclohexanone derivative **I** was combined with malononitrile and elemental sulfur under basic conditions to afford the aminothiophene **II** directly by the Gewald cyclization.[12] Acylation with the appropriate acid chloride under basic conditions afforded **3** or **5**. In a similar fashion, the isoxadiazole substituted aminothiophene antagonist **4** was prepared, as illustrated in Scheme 2. A Gewald cyclization on the the β-ketoester **III** with malononitrile afforded the aminothiophene **IV**. Acylation of this material with the appropriate acid chloride afforded the thiophene amide **V**. This intermediate was hydrolyzed to the corresponding carboxylic acid, followed by condensation with the hydroxamidine amide **VI** under standard coupling conditions to afford intermediate **VII** in good yield. Dehydration of this intermediate was accomplished by heating in diglyme, affording the isoxadiazole derivative **4**.

2.2. In vitro potency of glucagon receptor antagonists

The compounds were assayed by measurement of the inhibition of binding of ^{125}I-glucagon to the hGCGR expressed in CHO cell membrane, affording the binding IC_{50} values in Table 1. The compounds were further examined for the functional antagonist potency, as measured by the inhibition of glucagon-induced cAMP accumulation in hGCGR-transfected CHO cells (cAMP IC_{50}, Table 1). The peptide **1** is a potent glucagon receptor antagonist, with a binding IC_{50} of 18 ± 4 nM, and an equal potency in the functional assay with a cAMP IC_{50} of 26 ± 10 nM. The triaryl pyrrole antagonist **2** was reported previously from these laboratories.[9b] Although the compound retains similar inhibitory potency to **1** in the membrane-based binding assay (IC_{50} = 14 ± 5 nM), the compound is substantially less active as a functional antagonist of the glucagon receptor in the cell-based cAMP assay (IC_{50} = 120 ± 70 nM).[13] The thiophene-derived compounds **3**, **4**, and **5** have also been reported previously from these laboratories, and their potency in the binding and functional assays is presented in Table 1 for comparison.[11] The inactive thiophene derivative **5** was included in these NMR investigations as a structurally similar negative control. Finally, an additional class of potent antagonists are represented

Table 1. Binding and functional activity of antagonists of the human glucagon receptor

Compound		Glucagon in vitro assays (nM)[a]	
		Binding IC_{50}	cAMP IC_{50}
1	des-His_1[Glu_9]glucagon-NH_2	18 ± 4	26 ± 10
2	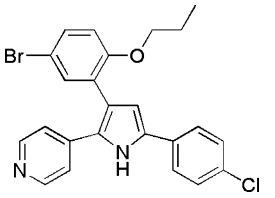	14 ± 5	120 ± 70
3[b]	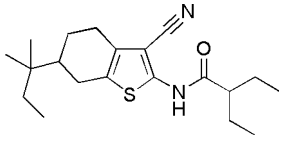	181 ± 10	129 ± 70
4	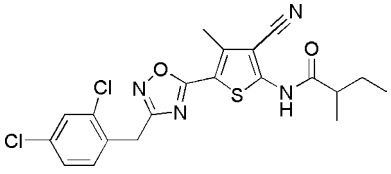	89 ± 17	34 ± 10
5[b]	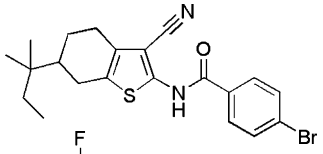	>10,000	>10,000
6	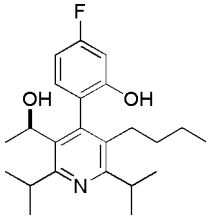	1.6 ± 0.2	0.7 ± 0.3
7	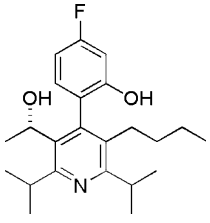	1270 ± 720	147 ± 50

[a] The IC_{50} values are given as means of three to four measurements ± SEM.
[b] Compounds were prepared and tested as racemic mixtures.

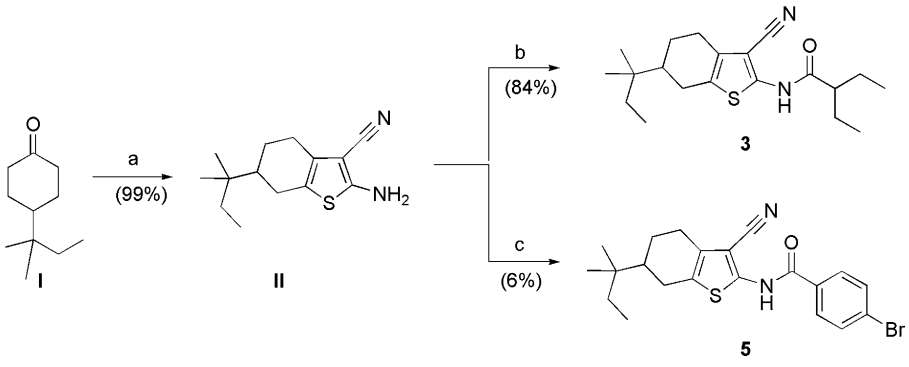

Scheme 1. Reagents and conditions: (a) malononitrile, S_8, morpholine, EtOH, 70 °C. (b) 2-Ethylbutyryl chloride, DIEA, CH_2Cl_2. (c) 4-Bromobenzoyl chloride, DIEA, CH_2Cl_2.

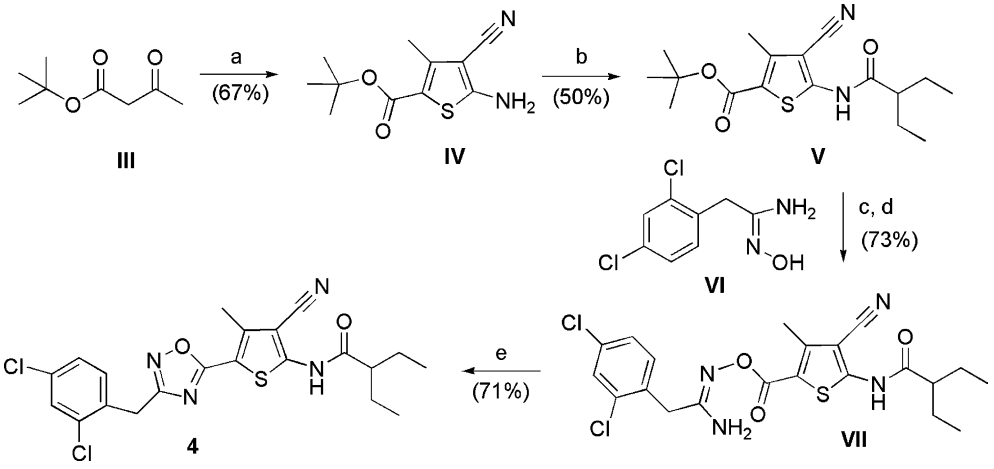

Scheme 2. Reagents and conditions: (a) malononitrile, S_8, morpholine, EtOH, 70 °C. (b) 2-Ethylbutyryl chloride, DIEA, CH_2Cl_2. (c) TFA, CH_2Cl_2. (d) EDC, HOBT, DIEA, DMF. (e) Diglyme, 135 °C.

by the recently reported phenylpyridine **6**.[10] The less active enantiomeric phenylpyridine **7** was also investigated in the liver NMR assay. The enantiomers **6** and **7** retain identical physical properties, but differ by over three orders of magnitude in their binding and functional potency in the hGCGR in vitro assays.[14] Thus, any difference in the efficacy of these compounds in the liver NMR assay may be ascribed directly to the difference in intrinsic potency of these compounds.

2.3. Perfused liver preparations and NMR measurements

The isolated perfused liver technique and the apparatus developed for liver perfusion in the NMR magnet have been described in detail previously,[7a,7c] and they are summarized here for clarity. As illustrated in Figure 1, perfused livers from hGCGR transgenic mice were surgically excised and positioned in a 20 mm NMR tube with the portal vein cannula suspended through the center of a modified Teflon plug. During the experiment, the Krebs buffer perfusion fluid containing dialyzed BSA was continuously oxygenated and recirculated through the liver. An initial 25 min period of flow-through, substrate-free perfusion washed out endogenous hormones and substrates. For absolute quantification of ^{13}C and ^{31}P metabolites, a reference compound reservoir was incorporated in the liver NMR perfusion cell; this reservoir contained methylenediphosphonic acid and [^{13}C]urea at effective amounts of 12 and 35 μmol, respectively.

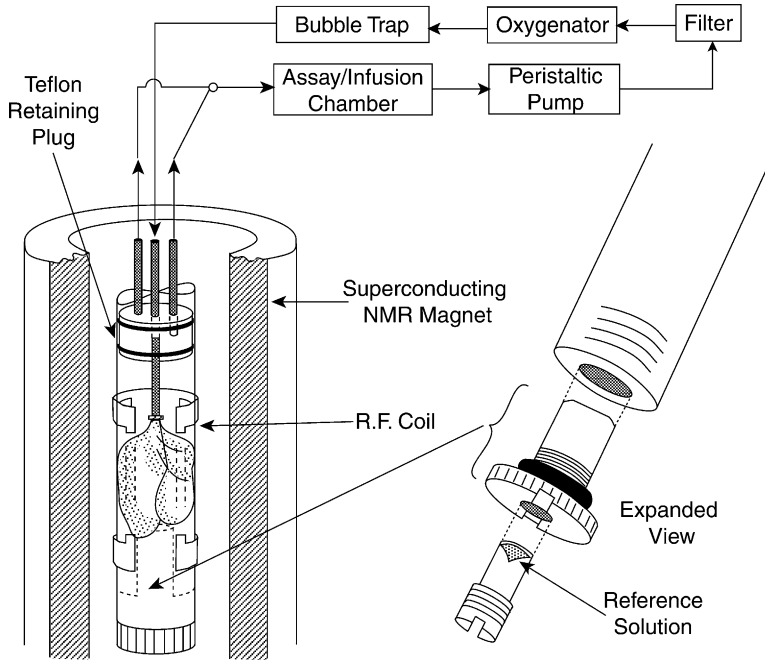

Figure 1. Essential components of perfusion of an isolated liver in the NMR magnet. Inflow of perfusion fluid is via the portal vein cannula. An expanded view of NMR perfusion cell (20-mm diameter) is shown on the right. The sealed referenced substance reservoir shown is described in the text.

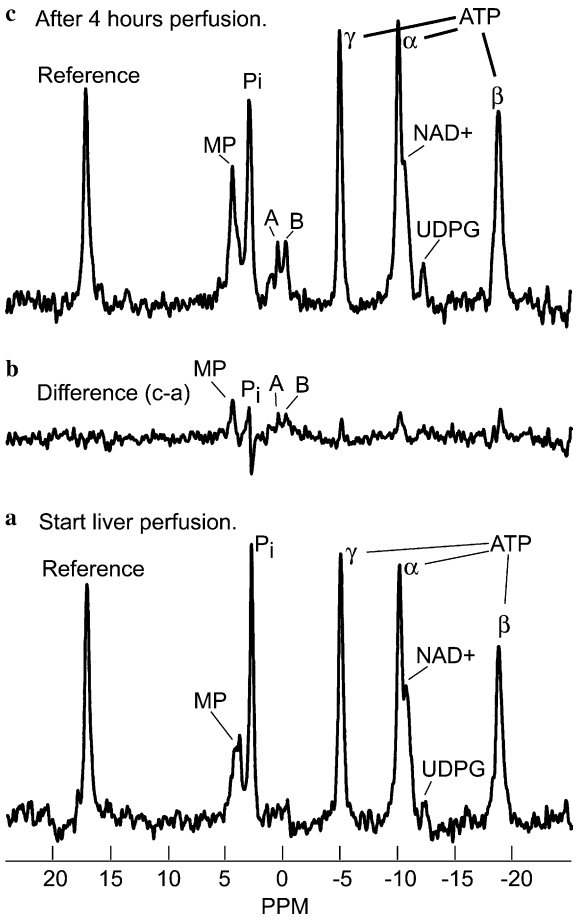

Figure 2. ^{31}P NMR spectra of isolated perfused hGCGR mouse liver at baseline (a) and 4 h later after accumulation of 18 ^{13}C spectra (c). The difference spectrum is shown in (b). This liver was exposed to 50 pM glucagon during the ^{13}C NMR phase.

2.3.1. Control studies of perfused liver NMR. ^{31}P NMR measurements. Only perfused liver preparations that were metabolically stable in the NMR magnet over the >4.5 h observation period were used in this study. One assessment of hepatic viability is stable and acceptable ATP levels over the course of the experiment; this was measured experimentally by ^{31}P NMR. A representative pair of ^{31}P NMR spectra from before and after an infusion experiment is illustrated in Figure 2. The bottom spectrum (a) shows a typical baseline profile of phosphometabolites in hGCGR mouse liver for which initial ATP = 3.3 μmol/g liver wet weight (glww). After 4 h perfusion (c) and after the addition of 50 pmol of glucagon under our NMR conditions, liver ATP levels remained constant (3.7 μmol/glww). Direct treatment with any one of the seven glucagon receptor antagonists studied did not affect hepatic ATP levels. Across the several treatments reported here, representative hepatic ATP levels were 3.6 μmol/glww ± 0.05 (N = 20, mean ± SEM), and the ratio of the ATP level measured after accumulation of all ^{13}C spectra to the ATP level measured at baseline was 0.99 ± 0.06 (mean ± SD).

2.3.2. Time-resolved ^{13}C NMR observations of hGCGR mouse liver. The biosynthesis of glycogen in the perfused liver was monitored by infusing the liver with the isotopically labeled (>99%) substrate [2-^{13}C]pyruvate using the apparatus illustrated in Figure 1. The ^{13}C isotopic label was incorporated into specific carbons of glucose-6-phosphate and eventually glycogen by the gluconeogenic pathway, illustrated in Scheme 3.[8a] Synthesis of glycogen and glucose at an acceptable, linear rate from substrates that enter the pathway at the level of pyruvate is a rigorous test of liver function. The kinetics of net glycogen synthesis were monitored in real time by measurement and integration of the discrete peak resulting from ^{13}C enrichment at C-1 of the glucosyl units in glycogen by ^{13}C NMR. As can be seen in Figure 3, glycogen C-1 (labeled peak A) gives rise to ^{13}C NMR signals free of overlapping peaks. Thus, hepatic metabolism was monitored under approximately metabolic and isotopic steady-state conditions

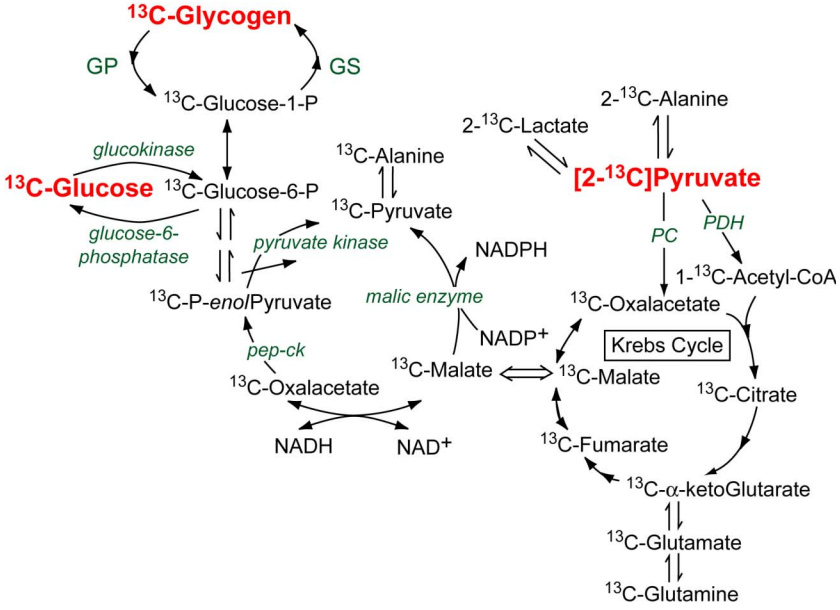

Scheme 3. Simplified gluconeogenic pathway monitored in perfused liver from exogenously administered [2-^{13}C]pyruvate to observed [^{13}C]glycogen and [^{13}C]glucose, shown in red. The key enzymes are shown in green.

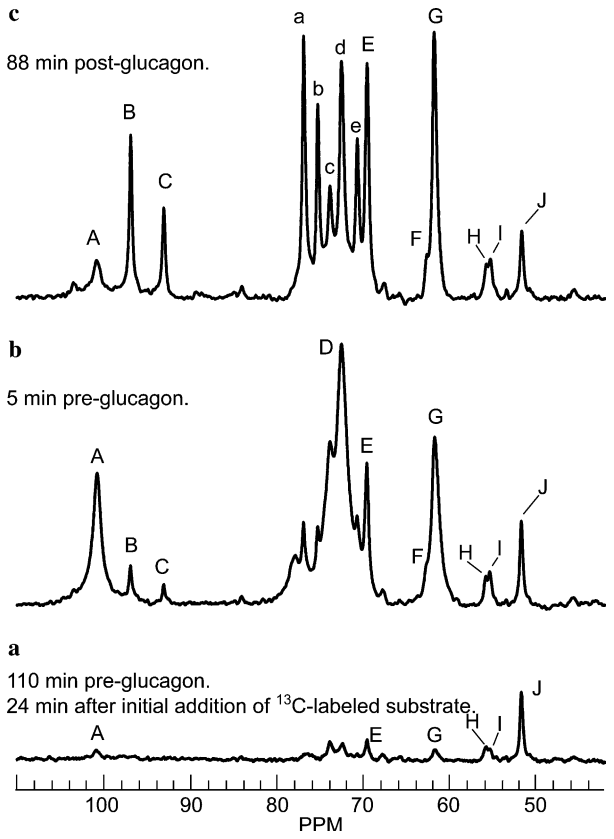

Figure 3. ^{13}C NMR spectra of a representative perfused liver from hGCGR mouse; (a and b) at the indicated times after the addition of [2-^{13}C]pyruvate and (c) after the subsequent addition of 50 pM glucagon. The spectral region 105–60 ppm contains signals of newly synthesized ^{13}C-labeled glycogen and glucose. The ^{13}C natural abundance background spectrum of the liver, measured under identical conditions before addition of ^{13}C-labeled substrate, was subtracted from each of the spectra shown. *Abbreviation:* (A) C-1 of glucosyl units of glycogen. (B and C) C-1 of β and α anomers of glucose. (D) C-2 to C-5 of glucosyl units in glycogen. (E) Lactate C-2 and C-2 of the glycerol backbone of triacylglycerols (TG). (F) C-1 and C-3 of TG glycerol. (G) C-6 of glucose and glucosyl units of glycogen. (H) Glutamate C-2. (I) Glutamine C-2. (J) Alanine C-2. (a–e) Correspond to signals arising from C-2 to C-5 of β and α anomers of D-glucose.[7]

by infusion of [2-^{13}C]pyruvate (6.7 mM) + NH_4Cl (2.7 mM). The biosynthesis of ^{13}C-labeled glycogen can be detected by ^{13}C NMR within 24 min of the addition of labeled substrate (Fig. 3a). [^{13}C]Glycogen is seen to accumulate monotonically in each subsequent spectrum for 105 min (Fig. 3b) as monitored by the glycogen C-1 signal (peak A). In control perfused livers maintained under these same steady-state conditions, newly synthesized [^{13}C]glycogen continues to accumulate for at least 3 h. However, administration of 50 pM glucagon to the perfused liver initiates an immediate cessation of glycogen accumulation, followed by the breakdown of the [^{13}C]glycogen synthesized to ^{13}C-labeled glucose (Fig. 3c). By subtracting the initial ^{13}C spectrum of the ^{13}C natural abundance of each liver from each spectra accumulated after the addition of ^{13}C-labeled substrate, only those signals that could be traced back directly to [2-^{13}C]pyruvate, such as [$^{13}C_1$]glycogen (Peak A), were selectively quantitated by integration.

The accumulation of [^{13}C]glycogen over time was measured by integration of the C-1 signal (Peak A in Fig. 3), and integration area versus time is plotted in Figure 4. Both groups of livers were treated with DMSO vehicle rather than a synthetic antagonist at *t* −25 min. One control group was treated with vehicle only, denoted as *no glucagon controls*. The rate of net accumulation of newly synthesized [^{13}C]glycogen in perfused hGCGR transgenic mouse livers was linear over 3 h in this group. In contrast, when the perfused livers were treated with vehicle plus 50 pM bolus of glucagon, a significant reduction of [^{13}C]glycogen was observed over the following 40 min. This control group is denoted as *DMSO + glucagon controls* in Figure 4. The rapid depletion of hepatic glycogen coupled with the appearance of ^{13}C-labeled glucose (Fig. 3) in this control group is attributed to glucagon-mediated glycogenolysis. The subsequent resynthesis of glycogen continues to be inhibited throughout the remainder of the experiment, from 40 to 80 min after glucagon addition.

2.3.3. Direct ^{13}C NMR observations of efficacy of glucagon receptor antagonists in hGCGR mouse liver. Addition of a glucagon receptor antagonist to the perfused liver prior to administration of glucagon was expected to diminish the subsequent reduction of [^{13}C]glycogen. As a validation of this NMR approach, perfused livers from our transgenic mice were treated with varying concentrations of the glucagon receptor antagonist peptide **1** 25 min prior to administration of glucagon. As illustrated in Figure 5, the presence of 1 μM of antagonist **1** almost completely blocked the induction of glycogenolysis by glucagon (Fig. 5b) and allowed the continued accumulation of newly synthesized [^{13}C]glycogen without appreciable buildup of ^{13}C-labeled glucose (Fig. 5c). The accumulation of [^{13}C]glycogen over time was again monitored by integration of the C-1 signal. The concentration-dependent inhibition of glucagon-induced glycogenolysis by **1**, as measured by these spectra, is illustrated in Figure 6.

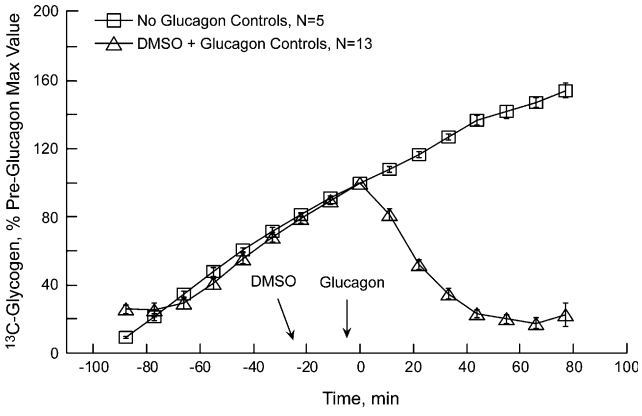

Figure 4. Quantitation of the accumulation of [^{13}C]glycogen in DMSO vehicle treated perfused liver from hGCGR mouse liver over 3 h (-□-). The effect of treatment with DMSO vehicle plus 50 pM glucagon (-△-) is also illustrated. Data represents the mean values and standard errors from the indicated number of hGCGR mouse perfused livers assayed.

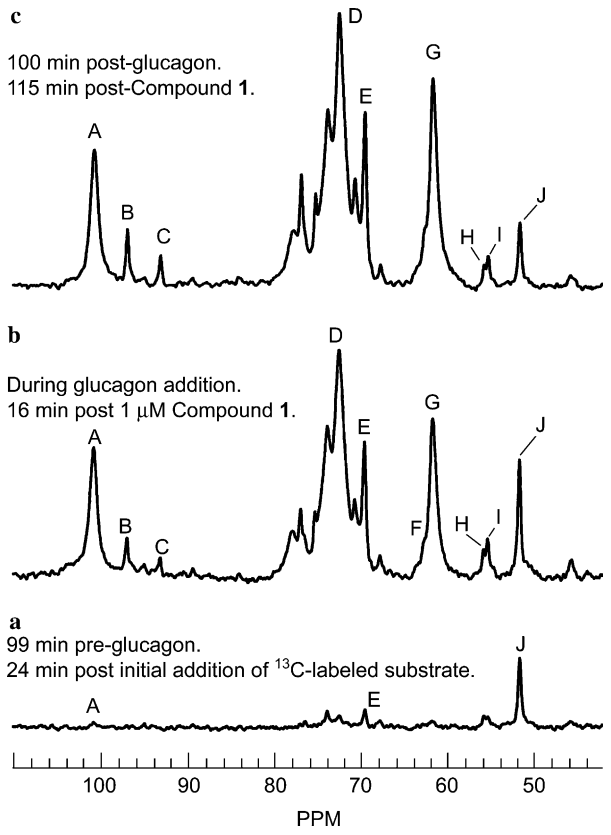

Figure 5. ^{13}C NMR spectra illustrating the action of the peptide glucagon receptor antagonist **1** in a representative perfused liver from and hGCGR mouse. Peptide **1** was administered at the indicated time prior to treatment with 50 pM glucagon under the conditions described in Section 5 of the text. NMR conditions and abbreviations are as denoted in Figure 3.

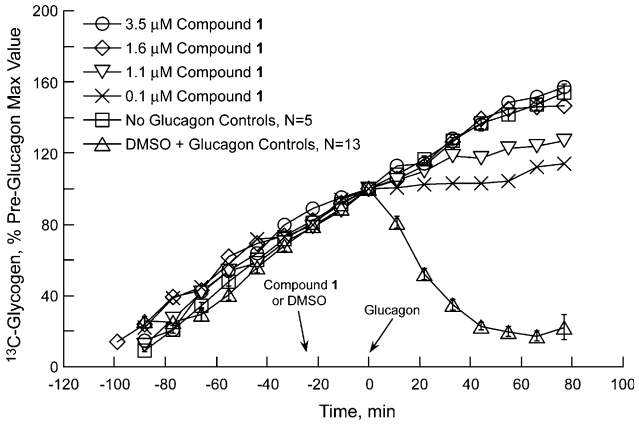

Figure 6. Quantitation of the inhibition of glucagon induced glycogenolysis by the peptide glucagon receptor antagonist **1** in perfused hGCGR mouse liver. Time of addition of glucagon, 50 pM, is designated as $t = 0$ min.

The control plots from Figure 4 are also presented for comparison. The peptide partially inhibits glucagon-mediated glycogenolysis at concentrations as low as 0.1 μM. At peptide concentrations above 1.1 μM glycogenolysis due to added glucagon is entirely eliminated.

The ^{13}C NMR integration plots from similar administration of the synthetic glucagon receptor antagonists **2** and **3** to perfused hGCGR mouse livers are illustrated in Figures 7a and b, respectively. Each compound mitigates the glycogenolysis due to glucagon in a concentration-dependent fashion, albeit at substantially higher concentrations than are required for a similar mitigation from the more potent peptide antagonist **1** (Fig. 6). The triarylpyrrole antagonist **2** afforded a near-complete impediment to glucagon-induced glycogenolysis at a concentration of 25 μM, whereas the thiophene-derived antagonist **3** only partially inhibited glycogenolysis at concentrations as high as 50 μM.

The activity of the more potent thiophene-derived glucagon receptor antagonist **4** is illustrated in Figure 8, along with the inactive thiophene derivative **5**. Again in this instance, the antagonist **4** effectively blocks glucagon-induced glycogenolysis in the transgenic hGCGR mouse livers in a concentration-dependent fashion. The structurally related thiophene **5** was inactive even at 50 μM, commensurate with the lack of activity observed with this compound in the in vitro glucagon assays (Table 1).

Finally, the activities of the potent phenylpyridine antagonist **6** and the less active enantiomer **7** are displayed in Figure 9. The glycogenolysis inhibition assay for **6** was measured twice at each concentration, and

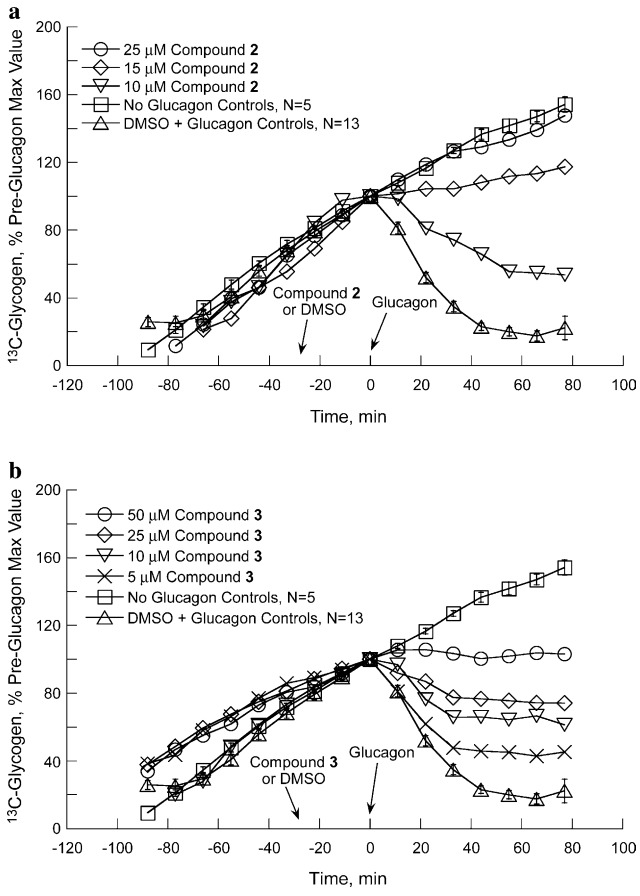

Figure 7. Concentration-dependent inhibition of glucagon induced glycogenolysis by synthetic glucagon antagonists **2** (a) and **3** (b) in perfused hGCGR mouse liver.

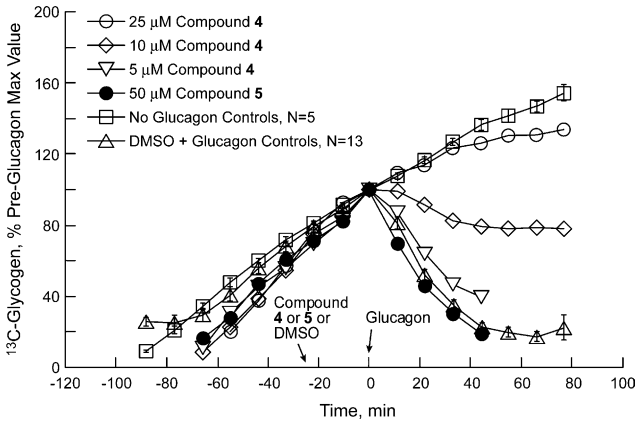

Figure 8. Concentration-dependent inhibition of glucagon induced glycogenolysis by synthetic glucagon antagonist **4**, and corresponding lack of inhibition by the inactive analogue **5**, in perfused hGCGR mouse liver.

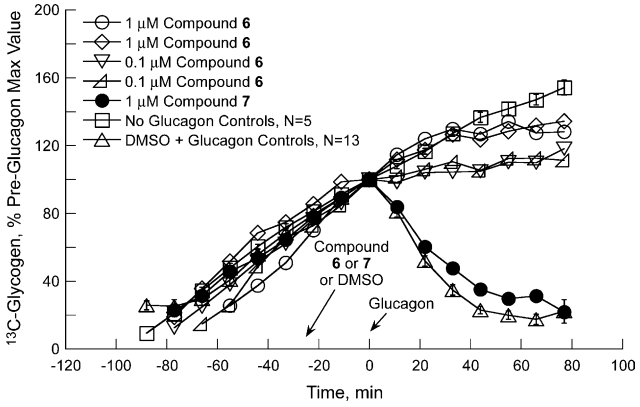

Figure 9. Concentration-dependent inhibition of glucagon induced glycogenolysis by synthetic glucagon antagonist **6**, and the substantially weaker inhibition by the less active enantiomer **7**, in perfused hGCGR mouse liver.

the data from the individual assays are plotted in Figure 9 as a measure of the reproducibility of the experiment between individual perfused livers. The potent phenylpyridine antagonist **6** afforded near-complete inhibition of glucagon-induced glycogenolysis at a concentration of 1 μM, whereas the less active enantiomer **7** afforded little inhibition at this concentration.

3. Discussion

The validation of activity of a chemical lead class toward a biological target represents one of the most formidable challenges in early lead development. Factors such as poor solubility, molecular aggregation, or chemical reactivity may conspire to produce artifactual activity in a cellular or membrane-based assay.[15] The confirmation of efficacy of chemical leads may be obtained by in vivo experiments, where the measurable pharmacological effect of a compound interaction with the biological target may be observed. However, the possibility of poor bioavailability or interfering biological interactions in the early examples of chemical lead class may hinder the interpretation of in vivo results. Thus, additional tools are needed that may demonstrate a pharmacological effect (or lack of effect) of exploratory compounds as early as possible in a medicinal chemistry lead optimization program.

In order to provide pharmacological validation for lead classes in our glucagon receptor antagonist program, we sought to remove as many barriers as possible to the observation of a direct pharmacological result of receptor antagonism. Species differences in receptor interactions with molecular antagonists were minimized by employing transgenic mice that express a functional human glucagon receptor. Furthermore, the variability of in vivo molecular exposure to the target of interest was minimized by examining the effect of the antagonists in the functioning organ ex vivo. The livers were exposed to 50 pM glucagon, which is approximately the physiological level of this hormone in vivo in wild-type mice.[16] Finally, the effect of the antagonist on the specific biochemical pathway of interest was examined by spectroscopically isolating this pathway for observation using ^{13}C-labeled substrate. In this way, the effect of novel classes of glucagon receptor antagonists could be demonstrated prior to optimization of other pharmacological properties.

The compounds studied in this investigation were chosen because they represent a variety of structural classes and a range of intrinsic potencies as glucagon receptor antagonists. Four separate structural classes of antagonists were examined in the perfused-liver NMR assay. The peptidyl antagonist **1**, the triarylpyrrole antagonist **2**, the aminothiophene antagonists **3** and **4**, and the phenylpyridine antagonist **6** all mitigated glucagon-induced glycogenolysis in a concentration-dependent fashion. The aminothiphene analogue **5** was inactive in the NMR assay, commensurate with the lack of activity of this compound in the binding and functional assays (Table 1). Similarly, while the potent phenylpyridine enantiomer **6** afforded near-complete inhibition of glycogenolysis at a concentration of 1 μM (Fig. 9), the less active phenylpyridine **7** afforded a substantially reduced inhibition of glycogenolysis at this concentration, commensurate with the diminished activity of **7** in the binding and functional assays (Table 1).

The ex vivo NMR assay may afford validation of a given lead class for pharmacological efficacy. However, the correlation of ex vivo glycogenolysis inhibition with in vitro potency is limited when comparing between two different lead classes. For example, the phenylpyridine antagonist **6** displayed a substantially greater intrinsic potency in the binding and cAMP assays than the peptide **1** (Table 1), but each afforded a similar inhibition of hepatic glycogenolysis at similar concentrations in perfused livers (Figs. 6 and 9).

The antagonists **2** and **3** exhibit similar activity in the liver NMR assay at concentrations of 10 μM (Fig. 7), but higher concentrations of **3** do not afford a concomitant increase in the inhibition of glycogenolysis. This disparity in activity between **2** and **3** at higher concentrations is

in contrast to the similar intrinsic potency exhibited by these antagonists in the cAMP assay (Table 1). The source of the discrepancies between the ex vivo liver assay and the in vitro functional assay is not entirely clear at present. During the course of the experiment, the perfusate solution containing substrate, glucagon, and antagonist was recirculated through the functioning hGCGR liver. It is possible that even under these controlled conditions the antagonists afford differing levels of accumulation in liver tissue, and this could be investigated using a modification of the tissue lysis methods reported by Dallas-Yang et al.[6b] Alternatively, differential rates of hepatic metabolism of the antagonists studied may be a factor affecting the direct comparison of compounds. The recirculating solution could be sampled and analyzed during the course of the experiment to account for this possibility, but such an analysis was not performed in the present study.

Notwithstanding the possibility of accumulation or hepatic metabolism of the compounds during the experiment, there are multiple additional variables that are absent in the ex vivo liver preparation, but that would be introduced during in vivo pharmacodynamic experiments. For example, in vivo experiments are subjected to differences in molecular absorption and tissue distribution, and binding of compounds to components of plasma, and any of these may hinder the early validation of exploratory lead classes of glucagon receptor antagonists. Indeed, we have reported previously the capricious in vivo efficacy of **2**, **3**, and **4** in blocking glucagon-induced glucose elevation in mice.[9a,11] The perfused-liver NMR assay presented herein affords validation of these compounds as effective antagonists of the human glucagon receptor, in that they block glucagon-mediated glycogenolysis in a concentration-dependent fashion in the entire organ expressing the human variant of the biological target. This ex vivo assay is not intended to supplant the demonstration of pharmacodyamic efficacy in the drug discovery process. It serves to bridge the gap between the observation of in vitro activity of a lead class and the demonstration of efficacy in vivo.

One shortcoming of the NMR glycogenolysis assay is the relatively low throughput for optimization of compounds, and in this respect the assay is similar to in vivo pharmacodynamic assays. Animal-to-animal variability may also be a factor in the observed results, although within a given mouse strain the activities of the hepatic enzymes controlling flux through the gluconeogenic pathway tend to be closely similar for similarly treated animals.[7a–c,8a]

The plot from the control experiments in Figure 4 includes standard deviation error bars and number of experiments for each group. It is evident from the small size of the error bars in Figure 4 that the reproducibility of glycogen synthesis and glucagon-induced glycogenolysis in control livers was excellent over multiple experiments under these meticulously controlled conditions. The NMR integration plots involving glucagon receptor antagonists illustrated in Figures 6–8 represent a single hGCGR mouse liver for each concentration of each compound. Whereas excellent reproducibility was observed in multiple control experiments (Fig. 4), only limited duplicate concentration assays have been run with synthetic antagonists. In those instances where duplicate antagonist experiments were performed (Fig. 9), the NMR assay exhibits excellent reproducibility.

4. Conclusions

The hGCGR perfused-liver NMR experiment has been developed as an assay that affords the direct observation of the effect of novel glucagon receptor antagonists specifically on the intended biochemical pathway. The technique allows for the pharmacological validation of lead compounds in the entire organ of interest prior to the optimization of pharmacokinetic properties. By appropriate choice of the ^{13}C-labeled substrate, the biochemical pathway of interest was spectroscopically isolated for observation. The assay described here utilized perfused livers from transgenic mice expressing the human glucagon receptor, thus minimizing potential species variations in compound efficacy. This technique does not provide adequate quantitative data for an accurate comparison of compounds with the precision of in vitro assays. Rather, this assay system represents a new development for validating the activities of glucagon receptor antagonists under more physiological conditions.

5. Experimental

5.1. Chemistry

All reagents and chemicals used were of the highest purity commercially available and were used without further purification. ^1H NMR spectra and ^{13}C NMR spectra of synthetic compounds were recorded on a Varian InNova 500 MHz instrument in $CDCl_3$ or CD_3OD as specified. Low-resolution mass spectra (MS) were determined on a Micromass Platform liquid chromatography–mass spectrometer (LC–MS). High-resolution mass spectra were acquired from a Micromass Q-TOF quadropole-time-of-flight mass spectrometer. All MS experiments were performed using electrospray ionization in positive ion mode. Leucine enkephalin was applied as a lock-mass reference for accurate mass analysis. All synthetic intermediates and final products were purified to >96% chemical purity as indicated by LC–MS, HPLC–UV, and NMR. Silica gel chromatography was performed with a Biotage Horizon$^{(R)}$ Flash Chromatography system from Dyax, Inc. using the gradient solvent systems indicated as per the manufacturer's instructions. The peptidyl antagonist **1** is commercially available from Bachem Bioscience, King of Prussia, PA, USA. The triarylpyrrole antagonist **2** was synthesized as described previously.[9]

5.1.1. *N*-(3-Cyano-6-*tert*-pentyl-4,5,6,7-tetrahydro-1-benzothien-2-yl)cyclopentanecarboxamide (3)

5.1.1.1. Step A. 2-Amino-6-(1,1-dimethylpropyl)-4,5,6,7-tetrahydro-1-benzothiophene-3-carbonitrile (II). To a solution of 5.00 g (29.8 mmol) of 4-*tert*-pentylcyclohexanone in 20 mL ethanol at 0 °C was added 1.97 g (29.8 mmol)

of malononitrile, followed by 3.89 mL (44.6 mmol) of morpholine, then 1.90 g (59.5 mmol) of elemental sulfur. The mixture was warmed to ambient temperature and stirred for 16 h. The reaction was then concentrated and purified by flash chromatography (5–15% ethyl acetate in hexane gradient) affording 7.32 g (29.5 mmol) of the title compound as a beige solid (99%). ^{1}H NMR (500 MHz, $CDCl_3$) δ 4.57 (s, 2H), 2.66 (m, 1H), 2.49 (m, 1H), 2.44 (m, 1H), 2.32 (m, 1H), 1.97 (m, 1H), 1.63 (m, 1H), 1.35 (m, 2H), 0.89 (s, 3H), 0.87 (s, 3H), 8.85 (t, J = 7.5 Hz, 3H); ^{13}C NMR (125 MHz, $CDCl_3$) δ 160.3, 132.6, 121.7, 115.7, 88.7, 43.1, 35.1, 32.8, 25.8, 25.6, 24.3, 24.2, 23.6, 8.4; HRMS: calcd for $C_{14}H_{20}ON_2SH$: 249.142. Found: 249.140.

5.1.1.2. Step B. *N*-(3-Cyano-6-*tert*-pentyl-4,5,6,7-tetrahydro-1-benzothien-2-yl)cyclopentanecarboxamide (3). To a solution of 3.97 g (16.0 mmol) of 2-amino-6-(1,1-dimethylpropyl)-4,5,6,7-tetrahydro-1-benzothiophene-3- carbonitrile (**II**) in 100 mL CH_2Cl_2 was added 8.36 mL (48.1 mmol) of di-*iso*-propylethylamine, followed by 2.75 mL (20.0 mmol) of 2-ethylbutanoyl chloride. After 16 h at ambient temperature, the mixture was poured onto 300 mL of saturated aqueous $NaHCO_3$ and extracted with two 100 mL portions of CH_2Cl_2. The combined organic layers were dried (Na_2SO_4) and concentrated. Purification by flash chromatography (2–7% ethyl acetate in hexane gradient) afforded 4.65 g (13.4 mmol) of the title compound as an off-white solid (84%). ^{1}H NMR (500 MHz, $CDCl_3$) δ 8.45 (s, 1H), 2.76 (dd, J = 5.0 Hz, J = 16.5 Hz, 2H), 2.65 (dd, J = 5.0 Hz, J = 16.0 Hz, 2H), 2.50 (m, 2H), 2.41 (m, 2H), 2.24 (m, 2H), 2.04 (m, 2H), 1.73 (m, 3H), 1.64 (m, 4H), 1.35 (m, 4H), 0.95 (t, J = 7.5 Hz, 6H), 0.90 (d, J = 8.0 Hz, 4H), 0.852 (t, J = 7.5 Hz, 3H); ^{13}C NMR (125 MHz, $CDCl_3$) δ 174.7, 159.6, 156.6, 151.8, 145.1, 134.8, 134.5, 131.9, 129.7, 128.1, 116.4, 114.0, 97.1, 50.4, 34.3, 25.6, 14.9, 12.1; HRMS: calcd for $C_{20}H_{30}N_2OSH$: 347.216. Found: 347.217.

5.1.2. *N*-{3-Cyano-5-[3-(2,4-dichlorobenzyl)-1,2,4-oxadiazol-5-yl]-4-methyl-2-thienyl}-2-ethylbutanamide (4)

5.1.2.1. Step A. *tert*-Butyl 5-amino-4-cyano-3-methylthiophene-2-carboxylate (IV). To a solution of 4.98 mL (30.0 mmol) of *tert*-butyl acetoacetate in 30 mL ethanol was added 1.98 g (30.0 mmol) of malononitrile, followed by 3.92 mL (45.0 mmol) of morpholine, then 1.92 g (60 mmol) of elemental sulfur. The mixture was heated to 70 °C for 2.5 h, then cooled to ambient temperature and concentrated. Purification by flash chromatography (5–20% ethyl acetate in hexanes) afforded 4.81 g (20.2 mmol) of the title compound as an off-white solid (67%). ^{1}H NMR (500 MHz, $CDCl_3$) δ 5.20 (s, 2H), 2.49 (s, 3H), 1.55 (s, 9H); ^{13}C NMR (125 MHz, $CDCl_3$) δ 164.2, 161.6, 145.3, 114.8, 113.4, 92.9, 82.2, 28.6, 15.3; LC–MS (ES) *m/e* 183 (M+1 *tert*-butyl).

5.1.2.2. Step B. *tert*-Butyl 4-cyano-5-[(2-ethylbutanoyl)amino]-3-methylthiophene-2-carboxylate (V). To a solution of 4.81 g (20.2 mmol) of *tert*-butyl 5-amino-4-cyano-3-methylthiophene-2-carboxylate (**IV**) in 100 mL CH_2Cl_2 was added 10.5 mL (60.6 mmol) of di-*iso*-propylethylamine, followed by 3.45 mL (25.3 mmol) of 2-ethylbutanoyl chloride. After 16 h at ambient temperature,the mixture was poured onto 300 mL of saturated aqueous $NaHCO_3$ and extracted with two 200 mL portions of CH_2Cl_2. The combined organic layers were dried (Na_2SO_4) and concentrated. Purification by flash chromatography (2–7% ethyl acetate in hexanes) afforded 3.39 g (10.1 mmol) the title compound as a yellow solid (50%). ^{1}H NMR (500 MHz, $CDCl_3$) δ 9.04 (s, 1H), 2.61 (s, 3H), 2.38 (m, 1H), 1.78 (m, 2H), 1.68 (m, 2H), 1.58 (m, 9H), 0.98 (t, J = 7.5 Hz, 6H); ^{13}C NMR (125 MHz, $CDCl_3$) δ 174.4, 161.6, 151.5, 142.8, 120.4, 114.2, 82.5, 50.6, 28.5, 25.7, 14.6, 12.1; HRMS: calcd for $C_{17}H_{24}N_2O_3SH$: 337.159. Found: 337.157.

5.1.2.3. Step C. (1*Z*)-2-(2,4-Dichlorophenyl)-*N*′-hydroxyethanimidamide (VI). To a solution of 2.00 g (10.7 mmol) (2,4-dichlorophenyl)acetonitrile in 50 mL ethanol was added 3.75 mL (26.9 mmol) of triethylamine, followed by 1.64 g (23.7 mmol) of hydroxylamine hydrochloride. The mixture was heated to 100 °C for 2 h, then cooled to ambient temperature and concentrated. The residue was purified by flash chromatography (50–100% ethyl acetate in hexanes) affording 1.23 g (5.64 mmol) of the title compound as a white solid (53%). ^{1}H NMR (500 MHz, $CDCl_3$) δ 7.43 (d, J = 2.5 Hz, 1H), 7.32 (d, J = 8.0 Hz, 1H), 7.25 (dd, J = 2.0 Hz, J = 8.5 Hz, 1H), 4.61 (s, 3H), 3.60 (s, 2H); ^{13}C NMR (125 MHz, CD_3OD) δ 153.1, 134.8, 133.8, 133.1, 131.3, 128.8, 127.2, 33.9; HRMS: calcd for $C_8H_8Cl_2N_2OH$: 219.010. Found: 219.008.

5.1.2.4. Step E. *N*-{5-[({[(1*Z*)-1-Amino-2-(2,4-dichlorophenyl)-ethylidene]amino}-oxy)carbonyl]-3-cyano-4-methyl-2-thienyl}-2-ethylbutanamide (VII). To a solution of 3.35 g (1.00 mmol) of *tert*-butyl 4-cyano-5-[(2-ethylbutanoyl)amino]-3-methylthiophene-2-carboxylate (**V**) in 50 mL CH_2Cl_2 was added 20 mL trifluoroacetic acid. After 2 h at ambient temperature, the mixture was concentrated, affording 2.80 g (1.00 mmol) of the corresponding carboxylic acid as a white solid (100%). ^{1}H NMR (500 MHz, CD_3OD) δ 2.62 (m, 1H), 2.57 (s, 3H), 1.70 (m, 2H), 1.59 (m, 2H), 0.92 (t, J = 7.5 Hz); mass spectrum (ES) *m/e* 281 (M+1). To a solution of 1.58 g (0.56 mmol) of this intermediate in 100 mL dimethylformamide was added 1.23 g (0.56 mmol) of (1*Z*)-2-(2,4-dichlorophenyl)-*N*′-hydroxyethanimidamide (**VI**), followed by 2.90 mL (1.69 mmol) of di-*iso*-propylethylamine, 0.762 g (0.56 mmol) of 1-hydroxybenzotriazole, then 1.08 g (0.56 mmol) of *N*-(3-dimethylaminopropyl)-*N*′-ethylcarbodiimide hydrochloride. After 16 h at ambient temperature, the mixture was poured onto 300 mL of 0.5 M aqueous $NaHCO_3$ and extracted with 300 mL ethyl acetate. The organic layer was washed with brine, dried ($MgSO_4$), and concentrated. Purification by flash chromatography (15–35% ethyl acetate in hexanes) afforded 1.97 g (41.0 mmol) of the title compound as a yellow solid (73%). ^{1}H NMR (500 MHz, $CDCl_3$) δ 9.38 (s, 1H), 7.44 (d, J = 2.0 Hz, 1H), 7.42 (d, J = 18.5 Hz, 1H), 7.26 (dd, J = 2.0 Hz, J = 8.5 Hz, 1H), 4.91 (s, 2H), 3.75 (s, 2H), 2.67 (s, 3H), 2.43 (m, 1H), 1.76 (m, 2H), 1.67 (m, 2H), 0.97 (t, J = 7.5 Hz, 6H); ^{13}C NMR (125 MHz, $CDCl_3$) δ 163.1, 147.0, 132.6, 131.4, 131.0, 130.2, 129.3, 128.2, 114.8, 94.1, 43.0, 35.1, 32.9, 32.8, 25.4, 25.3, 24.6, 24.5, 24.3, 24.2, 23.6, 8.4; HRMS: calcd for $C_{21}H_{22}Cl_2N_4O_3SH$: 481.087. Found 481.084.

5.1.2.5. Step F. *N*-{3-Cyano-5-[3-(2,4-dichlorobenzyl)-1,2,4-oxadiazol-5-yl]-4-methyl-2-thienyl}-2-ethylbutanamide (4). A solution of 1.80 g (3.74 mmol) of *N*-{5-[({[(1*Z*)-1-amino-2-(2,4-dichlorophenyl)ethylidene]amino}oxy)carbonyl]-3-cyano-4-methyl-2-thienyl}-2-ethylbutanamide (**VII**) in 80 mL diglyme was heated to 135 °C for 16 h. The reaction was cooled to ambient temperature and concentrated. Purification of the residue by flash chromatography (5–15% ethyl acetate in hexanes) afforded 1.23 g (26.6 mmol) of the title compound as a white solid (71%). ^{1}H NMR (500 MHz, $CDCl_3$) δ 9.12 (s, 1H), 7.45 (d, J = 2.5 Hz, 1H), 7.33 (d, J = 8.0 Hz, 1H), 7.26 (dd, J = 2.5 Hz, J = 6.0 Hz, 1H), 4.24 (s, 2H), 2.69 (s, 3H), 2.40 (m, 1H), 1.79 (m, 2H), 1.69 (m, 2H), 0.98 (t, J = 7.5 Hz, 6H); ^{13}C NMR (125 MHz, $CDCl_3$) δ 174.3, 171.4, 168.6, 152.6, 141.1, 135.3, 134.1, 132.1, 129.8, 127.6, 115.3, 113.9, 112.7, 96.9, 50.6, 29.8, 25.6, 15.1, 12.1; HRMS: calcd for $C_{21}H_{20}Cl_2N_4O_2SH$: 463.076. Found: 463.076.

5.1.3. 4-Bromo-*N*-[3-cyano-6-(1,1-dimethylpropyl)-4,5,6,7-tetrahydro-1-benzothien-2-yl]benzamide (5). To a solution of 3.23 g (13.0 mmol) of 2-amino-6-(1,1-dimethylpropyl)-4,5,6,7-tetrahydro-1-benzothiophene-3-carbonitrile (**II**) in 100 mL CH_2Cl_2 was added 6.79 mL (39.1 mmol) if di-*iso*-propylethylamine, followed by 3.57 g (16.3 mmol) of 4-bromobenzoyl chloride. After 16 h at ambient temperature, the reaction was poured onto 200 mL of saturated aqueous $NaHCO_3$. The organic layer was dried (Na_2SO_4) and concentrated. Purification by flash chromatography afforded 0.340 g (0.787 mmol) of the title compound as a yellow solid (6%). ^{1}H NMR (500 MHz, $CDCl_3$) δ 9.05 (s, 1H), 7.83 (dd, J = 1.5 Hz, J = 6.5 Hz, 2H), 7.69 (dd, J = 2.0 Hz, J = 7.0 Hz, 2H), 2.77 (dd, J = 5.0 Hz, J = 16.5 Hz, 1H), 2.70 (dd, J = 4.5 Hz, J = 15.5 Hz, 1H), 2.52 (m, 2H), 2.37 (m, 1H), 2.04 (m, 1H), 1.65 (m, 1H), 1.40 (m, 2H), 0.92 (s, 3H), 0.91 (s, 3H), 0.87 (t, J = 8.0 Hz, 3H); ^{13}C NMR (125 MHz, $CDCl_3$) δ 162.9, 146.9, 132.6, 131.4, 130.9, 130.2, 129.2, 128.3, 114.7, 94.1, 43.0, 35.1, 32.8, 25.4, 25.3, 24.5, 24.3, 24.2, 23.6; HRMS: calcd for $C_{21}H_{23}BrN_2OSH$: 431.079 and 433.077. Found: 431.078 and 433.078.

5.2. Biology

Chinese hamster ovary (CHO) cells expressing the cloned human glucagon receptor (CHO-hGCGR) have been described.[17] [2-^{13}C]Pyruvate ($\geqslant$99%) isotopic purity was purchased from Cambridge Isotope Labs (Andover, MA). Glucagon (1–29) and des-His^1 [Glu^9]glucagon-NH_2 (**1**) were purchased from Bachem Bioscience (King of Prussia, PA, USA). Glucagon stock solutions were assayed using glucagon RIA kits purchased from Linco Research (St. Charles, MO, USA).

5.2.1. Glucagon receptor binding assay. To determine the binding affinity of selected compounds, 2 μg of cell membranes from the CHO-hGCGR cells was incubated with ^{125}I-glucagon (NEN) in a buffer containing 50 mM Tris·HCl, pH 7.5, 5 mM $MgCl_2$, 2 mM EDTA, 12% glycerol, and 200 μg wheat germ agglutinin coated PVT SPA beads (Amersham), ± compounds. Non-specific binding was determined in the same buffer in the presence of 1 μM unlabeled glucagon. After 4–12 h incubation at room temperature, the radioactivity bound to the cell membranes was determined in a scintillation counter (Microbeta®—Perkin-Elmer Life Sciences, Boston, MA). The IC_{50} values were calculated using nonlinear regression (curve fit) analysis assuming single site competition.

5.2.2. Adenylyl cyclase assay. cAMP levels in CHO-hGCGR were determined with the aid of an adenylyl cyclase assay kit (SMP-004B, Perkin-Elmer Life Sciences, Boston, MA) as per manufacturer's instructions. For assessment of the antagonistic activity, cells were incubated with compound or 5% DMSO (as a control) in Flash plates(R) coated with anti-cAMP antibodies for 30 min and then stimulated with glucagon (250 pM) for an additional 30 min. All incubations were performed at room temperature in a 1:1 mixture of stimulation buffer and cell resuspension buffer. The cell stimulation was stopped by addition of an equal amount of a detection buffer containing cell lysis agent and ^{125}I-labeled cAMP tracer. After 3–6 h of incubation at room temperature, the ^{125}I-cAMP bound to the plate was determined using a liquid scintillation counter (Microbeta®—Perkin-Elmer Life Sciences, Boston, MA) and used to quantitate the amount of cAMP present in each sample. The IC_{50} values were calculated using nonlinear regression (curve fit) analysis.

5.3. Animals

The perfused livers from male mice, 28–34 g, from the hGCGR replacement strain reported previously[6] were used in all NMR experiments. The animals used in these experiments were bred and housed within our facility, and received chow (Harlan Teklad 7012) and water ad libitum. Perfusion studies were initiated during the middle of the dark sequence of a 12-h/12-h lighting cycle. The use of animals was done under the purview of an Institutional Animal Care and Use Committee, and all applicable regulations and laws pertaining to the use of laboratory animals were followed.

5.4. Perfused liver preparations and NMR measurements

^{13}C and ^{31}P NMR spectra of perfused liver at 37 °C were measured at either 8.5 or 11.7 T (AM360WB or Avance 500WB NMR spectrometers, Bruker Instruments, Billerica, MA) using probes in which the main coil was double-tuned for both the ^{13}C and ^{31}P frequencies. First, four baseline ^{31}P spectra of the perfused liver, each 200 scans (8 min), were accumulated over the first 32 min. Second, one natural abundance ^{13}C spectrum of 800 scans was accumulated over 11 min. Third, initial addition of ^{13}C-labeled substrate was followed by accumulation of 17 additional ^{13}C spectra under isotopic steady-state conditions. After measurement of the final ^{13}C spectrum, two additional ^{31}P spectra were accumulated.

5.4.1. NMR observation of glucagon-mediated glycogen metabolism. In preliminary perfusions of transgenic GCGR murine livers (N = 20) under the same ^{13}C NMR conditions described above, glucagon was titrated

using one single concentration, between 20 and 70 pM, for each perfused liver to establish the minimum level of glucagon required to reproducibly induce almost complete glycogenolysis and inhibition of [^{13}C]glycogen accumulation (data not shown). Under these conditions, the optimum concentration was determined to be 50 pM glucagon; this concentration is approximately equivalent to the physiological level reported for wild-type mice in vivo.[16] In other similar preliminary perfused livers ($N = 5$), dimethylsulfoxide (DMSO) was titrated to establish the level of DMSO that had no effect on hepatic metabolism under these NMR conditions. The no-effect level was found to be 0.25% DMSO. Consequently, the non-peptide hGCGR antagonists **2**–**7** were prepared in stock solutions that provided for infusion of exactly 0.25% DMSO in all cases. For the quantitation of net [^{13}C]glycogen accumulation in perfused hGCGR mouse livers, peak areas in the ^{13}C NMR spectra were determined as described previously[8a] by fitting spectra to appropriate line shapes with subsequent integration using the CF module of NMR1 software or similar functions included in the Matlab software package. Absolute integral units, normalized as a percent of the maximum pre-glucagon value for the given liver, were used in comparing the area of the ^{13}C enrichment at C-1 of the glucosyl units in glycogen (peak A) in the perfused liver preparations.

Acknowledgments

We are very grateful to William Hagmann and Scott Edmondson for their assistance in the preparation of the manuscript and for numerous helpful discussions. We are also grateful to Falguni Patel for assistance in the characterization of compounds.

References and notes

1. (a) Zhang, B. B.; Moller, D. B. *Curr. Opin. Chem. Biol.* **2000**, *4*, 461; (b) Jiang, G.; Zhang, B. B. *Am. J. Physiol. Endocrinol. Metab.* **2003**, *284*, E671; (c) Morral, N. *Trends Endocrinol. Metab.* **2003**, *14*, 169.
2. Moller, D. E. *Nature* **2001**, *414*, 821.
3. (a) Kurukulasuriya, R.; Link, J. T.; Madar, D. J.; Pei, Z.; Rhode, J. J.; Richards, S. J.; Souers, A. J.; Szczepankiewicz, B. G. *Curr. Med. Chem.* **2003**, *10*, 99; (b) Kurukulasuriya, R.; Link, J. T.; Madar, D. J.; Pei, Z.; Richards, S. J.; Rhode, J. J.; Souers, A. J.; Szczepankiewicz, B. G. *Curr. Med. Chem.* **2003**, *10*, 123; (c) Sloop, K. W.; Michael, M. D. *Drugs Future* **2004**, *29*, 835.
4. (a) Unson, C. G.; Andreu, D.; Gurzenda, E. M.; Merrifield, R. B. *Proc. Natl. Acad. Sci. U.S.A.* **1987**, *84*, 4083; (b) Hruby, V. J.; Ahn, J.-M.; Trivedi, D. *Curr. Med. Chem.—Immunol. Endocr. Metab. Agents* **2001**, *1*, 199.
5. (a) Ling, A. *Drugs Future* **2002**, *27*, 987; (b) Ling, A. L.; Wasserman, J. I. *Expert Opin. Ther. Patents* **2003**, *13*, 1.
6. (a) Shiao, L.-L.; Cascieri, M. A.; Trumbauer, M.; Chen, H.; Sullivan, K. A. *Transgenic Res.* **1999**, *8*, 295; (b) Dallas-Yang, Q.; Shen, X.; Strowski, M.; Brady, E.; Saperstein, R.; Gibson, R. E.; Szalkowski, D.; Candelore, M. R.; Fenyk-Melody, J. E.; Parmee, E. R.; Zhang, B. B.; Jiang, G. *Eur. J. Pharmacol.* **2004**, *501*, 225.
7. (a) Cohen, S. M. *J. Biol. Chem.* **1983**, *258*, 14294; (b) Cohen, S. M. *Biochemistry* **1987**, *26*, 563; (c) Cohen, S. M. In *Research in Perfused Liver: Clinical and Basic Applications*; Ballet, F., Thurman, R. G., Eds.; John Libby: London, 1991, Chapter 4; (d) Bergans, N.; Dresselaers, T.; Vanhamme, L.; Van Henke, P.; Van Huffel, S.; Vanstapel, F. *NMR Biomed.* **2003**, *16*, 36.
8. (a) Cohen, S. M.; Werrmann, J. G.; Tota, M. R. *Proc. Natl. Acad. Sci. U.S.A.* **1998**, *95*, 7385; (b) Cohen, S. M. *Anal. N.Y. Acad. Sci.* **1987**, *508*, 109.
9. (a) Cascieri, M. A.; Koch, G. E.; Ber, E.; Sadowski, S. J.; Louizides, D.; de Laszlo, S. E.; Hacker, C.; Hagmann, W. K.; MacCoss, M.; Chicchi, G. G.; Vivario, P. P. *J. Biol. Chem.* **1999**, *274*, 8694; (b) de Laszlo, S. E.; Hacker, C.; Li, B.; Kim, D.; MacCoss, M.; Mantlo, N.; Pivnichny, J. V.; Colwell, L.; Koch, G. E.; Cascieri, M. A.; Hagmann, W. K. *Bioorg. Med. Chem. Lett.* **1999**, *9*, 641.
10. Ladouceur, G. H.; Cook, J. H.; Hertzog, D. H.; Jones, H.; Hunertmark, T.; Korpusik, M.; Lease, T. G.; Livingston, J. N.; MacDougall, M. L.; Osterhout, M. H.; Phelan, K.; Romero, R. H.; Schoen, W. R.; Shao, C.; Smith, R. *Bioorg. Med. Chem. Lett.* **2002**, *12*, 3421.
11. (a) Qureshi, S. A.; Candelore, M. R.; Xie, D.; Yang, X.; Tota, L. M.; Ding, V. D.-H.; Li, Z.; Bansal, A.; Miller, C.; Cohen, S.; Jiang, G.; Brady, E.; Saperstein, R.; Duffy, J. L.; Tata, J. R.; Chapman, K. T.; Moller, D. E.; Zhang, B. B. *Diabetes* **2004**, *53*, 3267; (b) Duffy, J. L.; Kirk, B. A.; Konteatis, Z.; Campbell, E. L.; Liang, R.; Brady, E. J.; Candelore, M. R.; Ding, V. D.-H.; Jiang, G.; Liu, F.; Qureshi, S. A.; Saperstein, R.; Szalkowski, D.; Tong, S.; Tota, L. M.; Xie, D.; Yang, X.; Zafian, P.; Zheng, S.; Chapman, K. T.; Zhang, B. B.; Tata, J. R. *Bioorg. Med. Chem. Lett.* **2005**, *15*, 1401.
12. For a review of this method, see: Sabnis, R. W.; Rangnekar, D. W.; Sonawane, N. D. *J. Heterocycl. Chem.* **1999**, *36*, 3333.
13. Previous accounts from these laboratories (Ref. 9) reported a marked decrease in binding potency of compound **2** in the presence of 5 mM Mg^{2+} in a whole cell (filtration) binding assay, which effected a shift in the binding IC_{50} from 7 nM ($-Mg^{2+}$) to 170 nM ($+Mg^{2+}$). This dependence was not observed in the present membrane-based SPA-binding assay described in Section 5, which is run in the presence of 5 mM Mg^{2+}. The source of the discrepancy in Mg^{2+} dependence between the two assay formats is not fully understood at present. The functional antagonist activity reported here (cAMP $IC_{50} = 120$ nM) is in moderate agreement with that reported using a previous cell line and version of the functional assay (cAMP $IC_{50} = 41$ nM, Ref. 9b). For the sake of consistency, all activity values reported in Table 1 were derived from the present assay methods and cell lines as described in Section 5.
14. The binding IC_{50} values determined for **6** and **7** are sixfold more potent than the values reported in Ref. 10 for these compounds. The cAMP IC_{50} value determined for **6** is ninefold more potent that the value reported in Ref. 10, and a cAMP IC_{50} for **7** has not been previously reported. The discrepancies may be due to different cell lines used for the assays in Table 1 as compared to those used in Ref. 10. For the sake of consistency, all activity values reported in Table 1 were derived from the present assay methods and cell lines as described in Section 5.
15. McGovern, S. L.; Caselli, E.; Grigorieff, N.; Shoichet, B. K. *J. Med. Chem.* **2002**, *45*, 1712.
16. Parker, J. C.; Andrews, K. M.; Allen, M. R.; Stock, J. L.; McNeish, J. D. *Biochem. Biophys. Res. Commun.* **2002**, *290*, 839.
17. Chicchi, G. C.; Graziano, M. P.; Koch, G.; Hey, P.; Sullivan, K.; Vivario, P. P.; Cascieri, M. A. *J. Biol. Chem.* **1997**, *272*, 7765.